

Design of a Near-Ideal Fault-Tolerant Routing Algorithm for Network-on-Chip-Based Multicores

Costas Iordanou^{*}, Vassos Soteriou[†], Konstantinos Aisopos[‡]

^{*}Telematics Engineering
Universidad Carlos III de Madrid
and Telefonica I+D, Barcelona
kostas.iordanou@telefonica.com

[†]Department of EECEI
Cyprus University of Technology
vassos.soteriou@cut.ac.cy

[‡]Google
Mountain View, CA
kaisopos@gmail.com

Abstract—With relentless CMOS technology downsizing Networks-on-Chips (NoCs) are inescapably experiencing escalating susceptibility to wearout and reduced reliability. While faults in processors and memories may be masked via redundancy, or mitigated via techniques such as task migration, NoCs are especially vulnerable to hardware faults as a single link breakdown may cause inter-tile communication to halt indefinitely, rendering the whole multicore chip inoperable. As such, NoCs impose the risk of becoming the pivotal point of failure in chip multicores that utilize them. Aiming towards seamless NoC operation in the presence of faulty links we propose Hermes, a near-ideal fault-tolerant routing algorithm that meets the objectives of exhibiting high levels of robustness, operating in a distributed mode, guaranteeing freedom from deadlocks, and evening-out traffic, among many. Hermes is a limited-overhead deadlock-free hybrid routing algorithm, utilizing load-balancing routing on fault-free paths to sustain high-throughput, while providing pre-reconfigured escape path selection in the vicinity of faults. Under such online mechanisms, Hermes’s performance degrades gracefully with increasing faulty link counts, a crucially desirable response lacking in prior-art. Additionally, Hermes identifies non-communicating network partitions in scenarios where faulty links are topologically densely distributed such that packets being routed to physically isolated regions cause no network stagnation due to indefinite chained blockages starting at sub-network boundaries. An extensive experimental evaluation, including utilizing traffic workloads gathered from full-system chip multi-processor simulations, shows that Hermes improves network throughput by up to 3× when compared against the state-of-the-art. Further, hardware synthesis results prove Hermes’s efficacy.

I. INTRODUCTION

Multicore chips such as Chip Multi-Processors (CMPs) [36] employ Networks-on-Chips (NoCs) as their interconnect architecture of choice to provide efficient on-chip communication. Unfortunately, at deep sub-micron scales on-chip components become increasingly unreliable and susceptible to permanent faults, with the International Technology Roadmap for Semiconductors (ITRS) [33] projecting a 10-fold increase in CMOS wear rate in a 10-year span, while other studies pessimistically forecast that in future multi-billion transistor chips 20% of the transistors will be mal-produced with a further 10% failing during their lifetime [17]. While device failure rates will keep increasing at future CMOS technologies [5], multi-billion transistor chips containing faulty components will be expected to operate transparently as being reliable and fault-free [9].

In CMPs, transistors found in processing cores, cache memory, and on-chip network routers may equally fail permanently due to time-dependent physical wearout effects such as hot-carrier degradation and oxide breakdown [6], that may in turn quickly manifest to architectural-level failures. Individual core wear-out or failures in on-chip memory modules, however, may not be unavoidably disastrous to the CMP’s full-system functionality as cores and memory cells are inherently redundant to a particular extent [26]. Under such failure scenarios, the multicore system may preserve its functionality, albeit at a degraded performance mode, given that error detection and recovery techniques, such as fault-tolerant task migration, core- and cache-level error isolation and masking, and relevant operating system (OS) support, are available [18].

NoC fabrics, however, enjoy crucially less redundancy compared to other multicore chip components. Even an isolated intra-router defect or a sole link failure can morph a regular topology into an arbitrary one with an unanticipated geometry. Hence, either physical connectivity among network nodes may not exist at all due to the presence of faulty links and/or routers, that may even cause entire sub-network regions to detach from each other forming distinct partitions, and/or the associated routing protocol may not be able to advance packets to their destinations due to protocol-level violations. Traffic-induced back-pressure, then, causes accumulated congestion, possible traffic stalls, and even the entire multicore system to halt indefinitely rendering it inoperable. Hence an NoC failure, can become the entire multicore system’s *single* fatal failure.

A. Hermes: Synopsis and Contributions

A key operational stress-induced wear mechanism in current and future CMOS technologies is electromigration (EM) that causes material deformations and consequently the loss of connections in a circuit [4]. The International Technology Roadmap for Semiconductors [33] assesses EM as the main cause of on-chip metal interconnect reliability loss, an anomaly that is amplified in high-speed/thermally-stressed NoC links.

In an effort to establish inter-router communication resilience and hence to sustain seamless NoC operation in the presence of faulty links, we propose Hermes¹, a highly robust distributed fault-tolerant routing algorithm that bypasses faulty

¹In Greek mythology Hermes was an Olympian God, who among many roles, he was protector and patron of travelers.

network paths/regions/areas at a gracefully performance-degrading mode with increasing faulty link counts. Hermes employs a dual-strategy routing function that is aware of the current topological region's health state. Upon a message's network injection and continuing downstream in areas encompassing healthy links only, by default Hermes utilizes either XY Dimension-Order Routing (DOR) or load-balancing O1TURN routing [34] to sustain high throughput. Once a faulty link is encountered Hermes switches to using pre-calculated routing information distributed at each router that unitedly serve in forming an escape trail that steers that message toward its destination. To enact the latter mode, Hermes employs a route-discovering strategy which preempts regular operation, during which each root-acting node broadcasts atomically route-finding flags that spread synchronously along a spanning tree following the Up*/Down* scheme to program said tables in all inner and leaf nodes with how they can reach that root [1]. All nodes deterministically in turn assume this root role, so that finally routing tables at every node contain route data on how to reach any other NoC node.

The Up*/Down* process is tailored to provide deadlock-free routing in a NoC fabric containing faulty links as it forms an acyclic spanning tree that interconnects all its nodes [11], [32]. Further, no switching from Up*/Down* to either DOR or O1TURN routing is permitted in Hermes so as to break channel dependencies and avoid inducing deadlocks (see proof in Section II-E). With new faulty link(s) appearing in the topology, current Up*/Down*-based routes are invalidated and new ones are reconfigured; as such the network is frozen and said route-discovering flag-scanning process is repeated, until a new NoC interconnectivity is calculated and all routing tables are relevantly updated. NoC operation is then resumed. We note that works which propose intra-router redundancy-based wear resilience, such as in buffers and router ports [15], equally pivotal to an NoC's operational robustness [21], are complementary and can be orthogonally applied to Hermes's scheme to further extend an NoC's operational lifetime.

Hermes is geared towards 2D mesh NoCs, and while its Up*/Down* faulty path discovering and routing reconfiguration process are based on Ariadne's elegant approach [1], it entails a number of extensions and distinct contributions:

- 1) Its *two synergistic routing functions*, i.e., XY with *Up/Down*, or O1TURN with *Up/Down*, achieve gracefully-degrading performance with a growing faulty link count (see Section IV) vs. prior-art [1], [22].
- 2) It illustrates that *Virtual Channel (VC) classification* with respect to a routing path's state, i.e., whether it contains healthy links only or faulty links as well, and as such usage of each VC class by a distinct pre-configured or pre-designed routing function, offers superior performance compared to the arbitrary use of unclassified VCs, i.e., all VCs servicing a *single* routing scheme irrespective of whether in-transit messages traverse fault-free paths or currently bypass faulty paths (see Section IV).
- 3) It is a *purely hardware-based approach* and does not employ variable execution time iterative software kernels that demand OS scheduling and processing hardware support to discover fault-free routes, that may interrupt

multicore chip operation [22]. Hermes's *deterministic-time reconfiguration* implies *predictability* in network behavior ensuring an expected level of performance attainment as network down-time is strictly bounded [25].

- 4) Hermes *identifies network segmentations* using its topology-scanning flags. The OS running on a CMP may utilize this information to mark sub-network borders, enabling the assignment of independent processes and threads to each network partition [9] (see Section II-D).

An *ideal Fault-Tolerant (FT) routing algorithm* is defined as one that provides low-complexity all-to-all node connectivity given a fully-connected topology, while guaranteeing deadlock- and livelock-freedom during routing, and where its attainable throughput degrades in direct proportion to the lost aggregated bandwidth due to interconnect links failing. We claim that Hermes is a *near-ideal FT routing algorithm* as it meets all said goals, however, while its sustained throughput degrades gracefully with increasing faulty link counts (see Section IV-D) it drops at a slightly higher rate compared to the proportional loss in total link bandwidth. The latter occurs as link faults may not spread evenly across network space, or because they may lie at critical points such as at the network bisection, and crucially, due to the fact that in an attempt to establish freedom from deadlocks in a decimated topology some healthy links may not be utilized by the acyclic spanning trees that were reconfigured during Up*/Down* marking.

B. Hermes's Major Features and Attributes

Being near-ideal, Hermes possesses all the following *features* and meets all design *objectives* of a well-designed FT routing protocol [38], along with *extra attributes* (pts. 5 - 6):

- 1) It establishes *fault-tolerance* bypassing a *high number of faulty links* that can form any fault region (set of neighboring links) with no faulty link spatial placement restrictions and healthy link victimization to strictly adhere to geometrical rules in achieving protocol-level deadlock-freedom vs. works such as [12], [38]. Given a *realistic* minimally-connected path scenario, Hermes maintains *feasibility* in packet delivery given that *any* physical connectivity exists (see Section II). Hence, Hermes *adapts* to the state of the topology, where any spatial permutation of healthy and faulty links may exist.
- 2) It is *deadlock-free*, where no packets can be involved in a deadlocked situation which can halt the flow of packets and stall CMP operation indefinitely (see Section II-E), while establishing *short routes*, devoid of *livelocks*.
- 3) It is *distributed*, where each node individually directs its packets towards their next-hop router, with no expensive global information maintenance concerning the number and spatial distribution of faulty links (see Section II).
- 4) It supports *load-balancing* in fault-free regions to maintain high performance *irrespective of application spatio-temporal traffic behavior* (see Section II); it does not require explicit offline path analysis when more links fail, or when new applications are scheduled to run, to calculate specific topological bandwidth demands so as to tune channel selection to profiled traffic patterns [20].

- 5) It is *lightweight*, demanding *reasonable area and power overheads*, while keeping the base pipelined wormhole router's *critical path unaffected* (see Section IV-F).
- 6) It can handle *dynamically-occurring (run-time) link faults*; both transient and permanent faults can be handled, with Hermes geared toward the latter category.

Although in most previous works some of the above objectives can conflict each other [7], [12], [38], to our best knowledge Hermes may be the *first* FT routing algorithm for NoCs to *satisfy all of them*. Our experimental evaluation, including utilizing traffic benchmarks gathered from full-system chip multi-processor simulations, shows that Hermes reduces network latency and improves throughput by up to $3\times$ when compared against the state-of-the-art.

Next, Section II details Hermes's network reconfiguration scheme, routing algorithm and sub-network detection mechanism while Section III presents its micro-architecture. Following, Section IV evaluates Hermes, while Section V discusses related work. Finally, Section VI concludes this paper.

II. HERMES ROUTING ALGORITHM

With a NoC link(s) becoming faulty network operation is temporarily halted and Hermes's reconfiguration process is initiated preemptively to discover and mark all such faulty links so that they can be bypassed by advancing messages once regular network operation resumes. Here, we assume that all gate-level faults in an NoC router are mapped as equivalent link-level faults [1]; hence gate-level faults that render portions of a router as non-functional are captured as link-level faults which ultimately inhibit inter-router communication.

Following Ariadne's reconfiguration scheme [1], route discovery utilizes *atomic* flag broadcasts emanating from each node that in turn assume root status, spreading synchronously from that root along an acyclic spanning tree. This connectivity search treats a sub-connected network as a graph where the pattern of said flag broadcasting conforms to Up*/Down* rules, a route marking scheme originally utilized in local area networks [32] (LANs) and topology-irregular networks of workstations [31], [35]. We adopt this Up*/Down* scheme to 2D meshes, the topology of choice in silicon-planar NoCs [36], to program routing tables found in all remaining nodes with how they can reach that root. When this entire orchestrated process is done, with all nodes assuming in turn root role in a time-slotted mode, the routing table of each node contains information on how to reach all other physically connected nodes. As such, full NoC routing connectivity is established.

Up*/Down* is chosen as its topology-agnostic mode forms *directed acyclic spanning trees* that interconnect all NoC nodes; route traversals devoid of such cyclic patterns set the necessary and sufficient condition in guaranteeing *deadlock-freedom* in wormhole networks [11], [12]. The entire path discovery process converges in exactly N^2 cycles in an N -node network, where, positively, this deterministic-time reconfiguration leads to predictability in network behavior which then implies an expected level of performance attainment as network down-time is strictly bounded. NoC operation then resumes until a new faulty link(s) appears; as such, the entire route-discovering process is repeated to reproduce fresh routing

paths relevant to the newly generated irregular topology. Any faults in a router's datapath which can block access to links even when being healthy, including upstream and downstream buffers, control logic, and intra-router crossbar connections, are regarded as an extension to the link(s) connected to them, inevitably designating that link(s) as also being unusable [22].

A. Routing in a Fault-Free Region

Hermes combines two network routing strategies. At packet injection in a completely fault-free topology or fault-free region, Hermes uses either DOR-XY, dubbed as *H-XY*, or partially adaptive O1TURN [34] routing, named *H-O1TURN*. Under H-O1TURN, upon network ingress, a packet utilizes either XY or YX routing with equal probability as a means of balancing network load. Either of these routing schemes is followed until a faulty link is encountered, where routing switches to pre-configured Up*/Down* routes *exclusively* utilized until the network egress port is reached. H-XY uses 2 Virtual Channels (VCs), one for XY and the second by Up*/Down*, while H-O1TURN uses 3 VCs, one for XY, the second for YX, and the last for Up*/Down*. To preclude the formation of cyclic dependencies between said routing schemes and hence to avoid the advent of protocol-induced deadlocks [11], no switching from Up*/Down* routes to either DOR or O1TURN routing is permitted (see Section II-E).

Hermes utilizes two variants of Up*/Down* routing: 1) bidirectional Up*/Down* as used in Ariadne [1], where a fault in a unidirectional link victimizes its paired opposite-directional link as also being faulty, and 2), the upgraded Up*/Down* scheme of uDIREC [22], forming two variants dubbed *H-uXY* and *H-uO1TURN*, that marks unidirectional faulty links independently, hence incurring no healthy link victimization. However, as uDIREC requires iterative software kernels to form unidirectional Up*/Down* paths, while Hermes is purely hardware-based, we next focus on employing Ariadne's Up*/Down* scheme [1]; H-uXY and H-uO1TURN are solely used for performance comparisons in Section IV.

B. Routing in a Faulty Region: Reconfiguration Algorithm

A packet switches to Up*/Down* routing (from XY or O1TURN) and occupies its associated VC, *only when* it encounters a faulty link in its path, and keeps following its rules until its ejection to ensure deadlock-freedom (see Section II-E). The reconfiguration process begins upon the detection of a new faulty link(s), at which point the router to which this link is connected becomes the root node (initiator). As in numerous other FT approaches, we consider the presence of an online fault diagnosis/detection solution [24] that can promptly warn Hermes of erroneous NoC behavior. We also note that such fault-diagnosis/detection mechanisms are orthogonal to Hermes's route reconfiguration process.

As such, Hermes starts broadcasting Direction-Recoding Flags (*DRF*) to all of its output ports that engage a healthy link interconnecting to adjoining routers so as to *discover the topology's connectivity*. Flags are spread using a 2-bit overlay control network, which sits atop the data network, to ensure all-to-all node flag transmission/reception. The concept is that, upon reception of these DRF flags, the next-hop neighboring routers record the healthy input port through which the local

DRF had arrived into their routing tables so as to designate the direction (port) that leads them back to the root (broadcasting) node. Simultaneously (where applicable), Hermes broadcasts Alert Flags (AF) using the same control network to *discover network partitioning*, detailed next. Once a root node completes reconfiguration, the remaining nodes sequentially become root nodes, so that all nodes finally discover how to reach each other. Each node carries the following five-stage process (see Fig. 1), requiring control information bookkeeping and handling of reconfiguration orchestration among routers (stage actions 1 and 5, and AF flags are unique to Hermes, while stage actions 2-4 are inherited from Ariadne [1]):

- **Action 1. Flag/sub-network detection:** Identifies whether a node receives a DRF flag or an AF flag.
- **Action 2. Entering Recovery:** A network node enters recovery mode, invalidates its routing tables, freezes its pipeline and stops injecting traffic into the network.
- **Action 3. Tagging Link Directions:** Up*/Down* marks all adjacent links of a node as either “up” or “down.”
- **Action 4. Routing Table Update:** The routing table of the DRF-receiving node records the cardinal direction through which the current broadcasting node is reached.
- **Action 5. Flag Forwarding:** Forwards the reconfiguration flag according to the link status between each node-pair (healthy=DRF flag, faulty=AF flag). When a node is in recovering mode the AF flag is always ignored since the reconfiguration process has already begun.

When the root node completes broadcasting, the remaining $N - 1$ nodes singly broadcast their flags in a serial time-slotted mode. All five actions are carried out during the first broadcast, while only actions 4 and 5 are carried out during the remaining $N - 1$ broadcasts. Details of each action follow next.

Flag/Sub-Network Detection - Action 1: The 1-bit DRF and 1-bit AF flags are broadcasted from the root; DRF flags are propagated *atop healthy links only*, while AF flags are transmitted *atop faulty links only* via the 2-bit overlay control network (assumed to be always functional with triple modular redundancy) interconnecting routers. The use of DRF flags is to discover connected paths among all source-destination router pairs, while the AF flags mark possible boundaries of network partitions/segmentations (i.e., disjoint node clusters). As AF flags always follow *minimal* paths, while DRF flags may follow *non-minimal* paths due to the presence of faulty links, AF flags may arrive earlier at a router to *alert* the same router that it may possibly belong to a physically disconnected network segment. In case a router eventually receives a DRF flag from the root, while it had received an AF flag earlier, this ensures that a physical path emanating from the root does exist, and the AF flag is ignored canceling the previously set network segmentation alert. Otherwise, the node remains in its network segmentation alert mode (see Section II-D).

Entering Recovery - Action 2: Upon DRF flag reception, propagated from the current root node, the receiving node invalidates its routing table, freezes flit injection, stops its pipeline, and enters recovery. The state is set back to “normal” after N^2 cycles when the reconfiguration process is completed. Each subsequent DRF flag reception will only invoke Actions 4 and 5. However, in case the router had received an AF flag

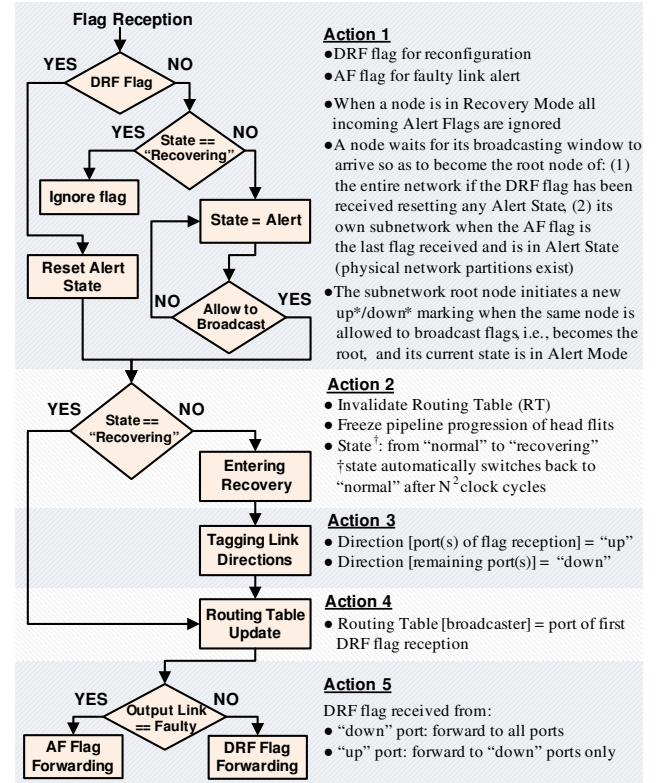


Fig. 1. Hermes reconfiguration algorithm.

and is in its alert state and not in recovery mode, by the end of the current N cycles it will be designated that this node belongs to a network partition. Since all nodes in all possible partitions will eventually broadcast, all boundaries among all partitions will eventually be discovered (see Section II-D).

Tagging Link Directions - Action 3: During this step, with the use of topology-propagating DRF flags, ports at a router are marked as either “up” or “down.” This ensures that all source-destination router pairs will eventually mark their routing tables with next-hop routes to be used to reach each other. The walk-through demo in Section II-D shows how DRF flags are propagated according to pre-specified rules which in addition maintain deadlock-free routing (see Section II-E).

Routing Table Update - Action 4: During each broadcast, a root node basically informs how it can be reached from all other nodes via the spreading of DRF flags that follows legal Up*/Down*-based turns (see Action 5); these DRF flag broadcasting patterns trail relevant paths starting from this root that are recorded, in a mirror-reflected mode, into each nodes’s routing table. Any node other than the root then uses these pre-recorded table paths to reach that root node.

Flag Forwarding - Action 5: Once the routing table of an intermediate node is updated, the same node broadcasts its DRF flag through those ports (via the 2-bit overlay control network) where the associated link is healthy, that it had not received a DRF flag from during the previous cycle, and it broadcasts an AF flag through the port(s) where the associated link is faulty. In addition, the Up*/Down* turn restrictions are also taken into consideration, that is, a DRF flag received from an “up” link is never sent to an “up” link; only “up” to “down” and “down” to “down” broadcasts are legal. In case where the link is faulty, no turn restrictions are applied, and the AF flag is sent atop the faulty link using the 2-bit overlay network to

the neighboring node. If the AF flag-receiving node is already in its recovering state then the AF flag is ignored (see Fig. 1).

C. Timing and Synchronization

Single-cycle flag forwarding among node pairs ensures that the broadcasting window of each node *deterministically* takes N clock cycles to complete, in an N -node topology. This considers the worst-case, but unrealistic, scenario of having a faulty topology that forms an exact *minimum spanning tree*, where N cycles are needed for a node's complete broadcast. Since each node broadcasts in a non time-overlapping *atomic* mode, reconfiguration takes N^2 cycles to complete; this scheme establishes determinism in network behavior, implying an expected level of performance attainment as network down-time is strictly bounded, while the entire reconfiguration process is exactly reproducible given a new faulty link occurrence.

D. Sub-Network Discovery Using AF Flags Walk-Through

During network reconfiguration, a root node is identified by all non-root nodes without explicitly forwarding its ID to them, as it is the sole flag originator during its broadcasting window. As such, *atomic* flag broadcasts [1] decoded in terms of correlating the system's global clock reference to a node's unique ID are employed in Hermes. This math formula states that the first $\log_2(N)$ LSBs of the global clock designate the broadcasting cycle of each root, while the next $\log_2(N)$ higher bits are used to identify the root node and hence its broadcasting slot; the latter commands exactly N repetitions (i.e., one for each node) using modulo arithmetic as $node((ID) \bmod(N))$ for node with identity ID , then $node((ID+1) \bmod(N))$ for node with identity $(ID+1)$ and so on until all N nodes become roots independently. Assuming an 8×8 NoC with 64 nodes, as in our experimental evaluation of Section IV, the first $\log_2(64) = 6$ LSBs and the next higher $\log_2(64) = 6$ bits of the global clock are used to designate the broadcasting cycle of each node, and the root node's ID, respectively. The Node ID Extractor (see Section III-B), a logic entity residing at every node, identifies the current root node and uses its ID to index the Fill Routing Table Logic (see Section III-A and Fig. 5-(b)) found in the same router so as to activate the one-hot 4-bit-long routing record associated with the current root. As such, the cardinal direction being serviced by each of the four input ports at a router dictate the relevant "up" or "down" bit setting of this specific record dictated by through-port-arriving DRF flags (see Section III). As such, every router's entire Up*/Down*-based routing table is eventually compiled. In case multiple concurrent faults occur, just one of the nodes becomes root according to the arbitrary current global clock value; all other nodes will eventually assume root status.

Fig. 2 walks through Up*/Down* marking and our Sub-Network Detection Mechanism (SNDM) that can detect individual network-dividing non-communicating partitions, using a 3×3 mesh. The former is served by the network-spreading single-bit DRF flags, and the latter by the single-bit AF flags. Both such flags span the network on a cycle-by-cycle basis using the 2-bit overlay control network (see Section II-B).

Fig. 2 emphasizes the usage of AF flags used by SNDM as they are a unique feature of Hermes, that traverse the topology along with DRF flags as in Ariadne's scheme [1]. In our

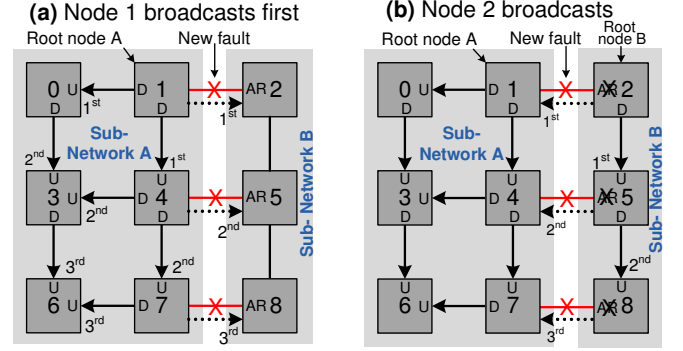


Fig. 2. A walk-through of Up*/Down* marking and the sub-network detection mechanism in a 3×3 mesh consisting of subnetworks A and B. AR denotes "Alert Register" is on, red lines with an "X" are broken links, solid and dotted lines show the broadcasting of the DRF and AF flags respectively at specified broadcast cycle times.

example, links $4 \leftrightarrow 5$ and $7 \leftrightarrow 8$ are initially faulty, while link $1 \leftrightarrow 2$ presently breaks down, partitioning the topology into sub-networks A and B. Instantly, node 1 acts as the root, initiates the reconfiguration process, enters recovery mode, and invalidates its current routing table entries. The broadcast cycle times of DRF and AF flags are shown at the side of each node, which begin spreading towards the vicinity of node 1 (see Section II-B). The purpose of AF flags is to label all links residing at the physical edges of sub-networks as border "guards" that mark and identify topological partitions.

As Fig. 2-(a) shows, node 1 marks its output ports connected to links $1 \rightarrow 0$ and $1 \rightarrow 4$ as "down" (D), and sends DRF flags to nodes 0 and 4. This sets their Status Register (SR) in recovering state (see Section III), where their respective input ports are set as "up" (U), with these port directions recorded into their respective routing tables. Nodes 0 and 3 are aware that node 1 is the root as the node ID is extracted from the global clock based on modulo arithmetic (see Section II-C), and hence all nodes are synced (Node ID Extractor of Section III-B). Node 2 only receives an AF flag, via the control network, since link $1 \leftrightarrow 2$ is now faulty, setting its Alert Register (AR) in alert state. Following Up*/Down* rules, in cycle 2 node 0 marks link $0 \rightarrow 3$ as D and U, and node 4 marks links $4 \rightarrow 3$ and $4 \rightarrow 7$ both as D and U, all at their two respective ends. Nodes 3 and 7 are set in recovery state, while node 4 sends an AF flag to node 5 atop $4 \leftrightarrow 5$ faulty link, via the 2-bit control network, setting node 5 in alert state. Finally, in cycle 3 the north and east ports of node 6 are marked U, setting node 6 in recovery state, while node 8 receives an AF flag from node 7 atop $7 \leftrightarrow 8$ faulty link setting node 8 in alert state. Now subnetwork A has completed both its Up*/Down* marking for all of its member nodes and recording of all paths which lead towards root node 1. Note that AF flags cause no Up*/Down* marking at the receiving nodes, since they merely designate the possibility of a network disconnection at the receiver node, and that no $U \rightarrow U$ marking is allowed to ensure acyclic behavior [31], [35]. Also, no node that receives a DRF or AF flag from one of its ports can later send any other flag using that same port so as to avoid erroneous port marking synchronization; flag reception time is tied to the global clock dictated by the Node ID Extractor (see Section III-B).

With $N = 9$ cycles elapsed, where N is the node count, node

2 broadcasts next, designated by the global clock utilized by the Node ID Extractor (see Section III-B), initiating a new Up*/Down* marking chain of events, shown in Fig 2-(b). The reception of an AF flag and no DRF flag by node 2 from the previous cycle, points towards its separate sub-network presence. Node 2 broadcasts its DRF and AF flags accordingly, following the flag-based Up*/Down* marking rules. The south port of node 2 is set as D while the north port of node 5 is set to U in cycle 1, and so on. However, when nodes 1, 4 and 7 receive an AF flag from corresponding nodes 2, 5 and 8 residing in sub-network B, they ignore this flag since they are already in recovering mode. Nodes 3-8 and 0 will broadcast in series as roots when their turn arrives, dictated by the global clock, where each informs its sub-network-residing nodes how they can be reached by broadcasting DRF flags.

The process completes in N^2 cycles with node 0 ending its broadcast. By then, *only valid escape paths* are recorded into the routing table of each router, reflecting upon routes that *are valid only within the same sub-network*, i.e., either in sub-network A or in sub-network B. This information may subsequently be provided to the operating system to mark the borders of these sub-networks, enabling the assignment of independent processes and threads to each such sub-network, being serviced by a sophisticated algorithm such as [9].

E. Hermes Deadlock Freedom: Discussion & Proof

We provide a short, yet comprehensive proof of deadlock-freedom present in the H-XY and H-O1TURN routing algorithms. We adopt Duato's theorems [10], [11] which have been instrumental in designing deadlock-free routing schemes for mesh-based off- and on-chip interconnection networks. Duato defines a deadlock-prone network as the one which contains cycles in its *extended channel dependency graph*. Hence, to prevent deadlocks *cyclic dependencies between channels have to be prohibited* during routing protocol design. Next, in Fault-Tolerant (FT) routing algorithms, connectivity, whose degree is determined by the presentence of faults at links (physical) in combination with the routing algorithm's reachability (by protocol), has to be considered in proving that a FT routing algorithm, such as Hermes, is free of deadlocks.

To prove that Hermes causes no deadlocks, we first consider each constituent routing scheme, i.e., DOR-XY (or, XY), O1TURN, and Up*/Down* individually, and show that each is free of cyclic channel dependencies in their context of traversed route health status. In a second step, we then constructively prove that the combination of XY and Up*/Down* in H-XY, and O1TURN with Up*/Down* in H-O1TURN, are devoid of cyclic channel dependencies and hence deadlocks.

For first prove that the XY (YX) and O1TURN algorithms are deadlock-free, despite being trivial in doing so. First XY makes turns from any horizontal to any vertical cartesian direction, totalling 4 turns. As such, forming overlapped abstract turns for the clockwise and anticlockwise directions one sees that no full cycles are possible, hence XY is devoid of deadlocks. Such analysis applies to YX routing too. Hence, one VC is sufficient to achieve deadlock-free DOR routing (XY or YX) in a mesh network [10]. Next, O1TURN is implemented with two (VCs) per physical channel (or port/link) where one

VC (or "layer" [34]) services XY and the other YX routing. Upon packet injection, there is a 50% chance in using either VC, where switching between VCs is prohibited and a packet uses the same VC until its network egress. Using an extended channel dependency graph [11], one sees that no cycles form between the two VCs: O1TURN routing is deadlock-free.

As discussed in Section II-B and shown in Section II-D, a well-orchestrated route discovery process executed in a distributed fashion by the augmented logic (see Section III) found in every NoC router using topology-spreading flags to *mark a loop-free assignment of direction to the operational NoC links* is triggered in the event of any link(s) becoming faulty, turning the regular mesh topology into an arbitrary one [29], [35]. This preemptive process fills every router's routing table with calculated routes to be used by traversing packets in regions where all faulty links must be bypassed, until their network egress; the algorithm is re-executed when future faults occur to replace current routes with newly calculated ones. The underlying principle of said link direction assignment is the spanning tree [32], with the "up" ("down") marking at each link designating the link end that is closer (farther) to the root of the tree. The result of this "up" to "down" assignment is that the directed links, and consequently all the spanning trees emanating from each root (source) node to every possible leaf (destination) node do not form loops, hence every spanning tree is acyclic. This Up*/Down* marking is guaranteed to form a *directed acyclic spanning tree* between any root-leaf node pair, as long as there is physical connection between them, or a series of directed healthy links. In Up*/Down* routing, the unique node order assignments to each router, where all increasing-order turns (down links) are disabled if followed by decreasing-order turns (up links), or vice-versa, ensure a unique visiting order where this decreasing to increasing node visiting order ensures the absence of cycles, i.e., a turn from "down" to "up" is illegal and hence prevented (self-looping at a node is also disallowed), thus eliminating full cyclic channel dependencies. Hence, the Up*/Down* scheme is deadlock-free, for no deadlock-producing loops are possible, as proven in [35], albeit for irregular fault-free networks².

Hermes's deadlock-freedom can be proven informally [35] by contradiction³ as follows: consider that there is a deadlocked configuration due to a cyclic channel dependency between either XY or YX and Up*/Down* routing, as messages are allowed to switch from either VC assigned for XY or YX usage to the VC belonging to Up*/Down*, and then back to the VC belonging to either XY or YX. In this configuration, messages cannot have switched to either XY or YX routing and associated VCs if the same messages had occupied the VC belonging to Up*/Down* routing as Hermes prohibits such a channel switch. Thus, all blocked messages must currently be occupying a VC belonging to either YX or XY. However, those protocol-deadlocked messages can bypass a faulty link lying in their minimal path, which would cause physical blockage, by using the VC belonging to Up*/Down*, as Up*/Down*

²Link faults transform a regular mesh topology into an irregular one, hence Up*/Down* in Hermes deals with irregular topologies as done in [35].

³Deadlock freedom in Hermes may be formally proved using the step-by-step process dictated in [11]; it is omitted here due to space limitations.

routing is by design deadlock-free, bypasses faulty links, and can deliver those messages to their destinations given lack of network partitioning. Hence, there cannot be a deadlocked configuration, both in terms of protocol effects and physical blockage due to the presence of a faulty link(s). As such, both H-XY and H-O1TURN Hermes variants are deadlock-free.

F. Maximum Number of Faulty Links Handled by Hermes

We model a NoC as a strongly connected directed mesh graph $G = (V, C)$ with node (router) set V and edge (link) set C with a total number of edges $|C| = \sum_{i=0}^{n-1} c_i$, where all such edges possess healthy status. A *minimum spanning tree* $S = (V, C')$ is an acyclic and connected sub-graph of G such that it connects *all* the *distinct* nodes in G via a path of finite sequence of edges of non-faulty status according to the Up*/Down* scheme marking rules in the form $v_0 \rightarrow v_1 \rightarrow \dots \rightarrow v_{m-2} \rightarrow v_{m-1}$ such that $c_0 \neq c_{m-1}$, i.e., S contains no cycles. Also, $n > m$ so that $C' \subset C$. Let F be the set of faulty edges in G so that $C' \cup F = \emptyset$ and $C = C' \cup F$. As such, the maximum number of faults that can be handled by Hermes is $|F| = |C| - |C'|$. For example, in an 8×8 mesh NoC, used in our experimental evaluation in Section IV, $|C| = 112$ and $|C'| = 63$; hence, $|F| = 49$ faulty bidirectional links (or, 43.8%) can be handled by Hermes at maximum with guaranteed packet delivery among all routers in a deadlock-free mode.

G. Breadth-First Search (BFS) vs. Depth-First Search (DFS)

Hermes utilizes BFS to scan the interconnect graph during Up*/Down* marking using DRF flags to build routing tables, as Fig. 3-(a) shows, where link $(0, 1) \leftrightarrow (1, 1)$ is faulty. BFS is very efficient when applied to regular topologies, e.g., meshes, due to the algorithm's fork-like spreading nature; as Fig. 3-(b) shows, it takes 4 cycles to search the entire graph starting from the root with cartesian coordinates $(0, 0)$. DFS can be highly inefficient when used in regular topologies as its search spreads linearly, requiring much more time to build a graph; as Fig. 3-(c) shows, when DFS is applied to the same mesh topology it takes 8 cycles to build the graph backbone (solid links in Fig. 3-(d)), while it recurses in order to build edges in the DFS graph that capture still undiscovered links, i.e., those dotted in Fig. 3-(d). As this is highly-dependent on the root's location [30], the exact convergence time is highly variable.

A major issue with Up*/Down*, however, is that depending on the spatial distribution and number of faults, it creates non-minimal routes in the quest of avoiding cyclic channel dependencies and hence deadlocks (see Section II-E). However longer paths point to an increase in the mean hop count of packets, hence latency is increased and the network's effective throughput is reduced. For these exact reasons, various works applicable to the domain of off-chip Networks of Workstations (NoWs) proposed either, (a) the relaxation of Up*/Down* in searching for routes and the later use of heuristics as inputs to iterative methods so as to break cycles [31], [35], or (b), the use of DFS in irregular NoWs in order to enact flexibility in constructing connectivity graphs so as to introduce previously unconsidered legal connections among routers that improve performance, by up to $3\times$, with shorter routes [30], [35].

Both such methods, however, exhibit performance gains that are highly dependent on the choice of initial root node,

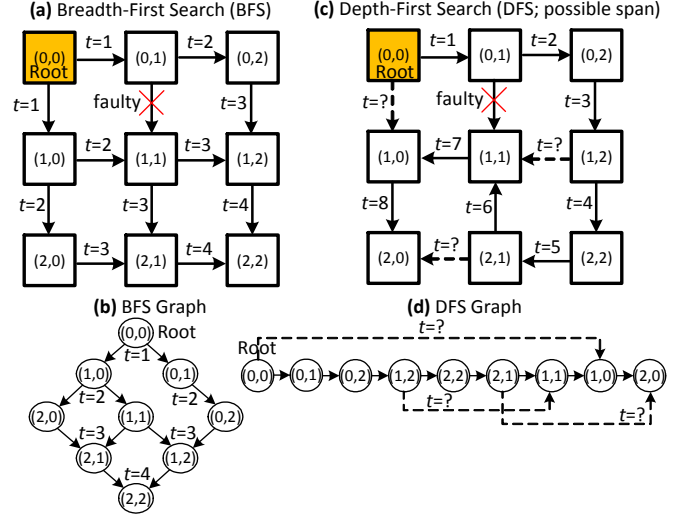


Fig. 3. A comparison of BFS vs DFS algorithms applied to a 3×3 mesh NoC. t indicates the search cycle where “?” means unknown.

are applicable to non-faulty networks, and require use of heuristics in tandem with recursive search, including trying out alternative root nodes during tree search. The latter two are implemented using augmented hardware that demand high overhead investment and/or using software tools and runtime OS kernels that are computationally expensive.

Despite the fact that Hermes deals with an irregular topology once a first link fault occurs, we argue that such said methods should not or cannot be applied to Hermes as they negate its very purpose: Hermes is a lightweight, purely hardware-based scheme suitable for resource-constrained NoCs, it does not require recursive software methods to discover routes and it is thus computationally oblivious, it rotationally designates all nodes as acting roots when performing Up*/Down* graph search, hence no optimization in root choice may be applied, and given its near-ideal FT routing nature it dictates deterministic-time reconfiguration (see Section II). Yet, Hermes is flexible as it can be used in software-based iterative methods, demonstrated with our construction and testing of H-uXY and H-uO1TURN scheme variants (see Section IV).

III. HERMES MICRO-ARCHITECTURE

Hermes uses a 4-stage pipelined wormhole NoC router with 3 input Virtual Channels (VCs), comprising (1) routing computation, (2) VC arbitration, (3) switch allocation, and (4) crossbar traversal⁴. Inter-router link traversal consumes 1 cycle. Fig. 4 depicts Hermes's router micro-architecture that incorporates added circuitry required for Hermes's operation.

Hermes's Fill Routing Logic Tables unit, shown in Fig. 4, is divided into three sub-blocks, comprising Up*/Down*, DOR-XY and DOR-YX routing, each utilizing a separate VC. H-XY routing utilizes the first two blocks, while H-O1TURN utilizes all three blocks where XY or YX routing are used with equal probability when routing in a fault-free region. The Up*/Down* block is directly connected to Hermes's logic unit which provides next-hop routing information, as Fig. 5-(b) shows, stored in routing tables, and is employed when the

⁴Hermes is orthogonal to other existing pipelined NoC router architectures such as the speculative wormhole architecture in [23].

current packet being routed has encountered a faulty link in its progressive path. These routing tables are updated every time a new faulty link(s) appears in the network, dictated by the route reconfiguration algorithmic process described in Section II-B. The VC Allocator assigns the sole VC governed by Up*/Down* routing to a packet being routed in a faulty region, up until that packet reaches its destination to maintain deadlock-freedom (see Section II-E); otherwise XY's VC is assigned under H-XY, or either of the XY or YX VCs are utilized in H-OITURN when traversing a fault-free region.

Fig. 4 shows Hermes's various logic components comprising the 1-bit Status Register (SR) with "normal" and "recovering" states, the 1-bit Alert Register (AR) with 'normal' and "alert" states, four 1-bit registers to designate "up" or "down" routing (one for each port) when Up*/Down* is in use, the logic to update the SR and AR registers accordingly (Action 3; see Section II-B), to fill the routing tables (Action 4), and to forward the DRF or AF flags (Action 5). Hermes's router has sixteen 1-bit width wires for flag reception and forwarding, shown as $flag_{0-3}(in)$ and $flag_{0-3}(out)$ for flag in and out signals. Each $flag(in)$ or $flag(out)$ pair at each port consists of two 1-bit wires, one for each DRF and AF flag forwarding.

The SR holds the current state of the network, where "recovering" implies that the network is currently stalled to reconfigure the routing tables, and where "normal" implies that the network is operating normally or it has resumed normal operation after completing its routing table reconfiguration process as a response to fault(s) recovery. Under the normal state packets can be injected into the network since valid routing paths exist in the routing table of all NoC routers. The AR is updated as follows: if a new AF flag is received and the SR is in the "normal" state, then the AR register is set to the "alert state." If an AF flag is received under a current recovering state, then the AF flag is ignored. If the AF flag had already been received and the AR register is currently in the "alert" mode, then if a DRF flag is also received, the AR is reset to the "normal" state (see Section II-B and Section II-D).

A. Hermes's Router Logic Blocks

When the SR is in recovering state, the signal which freezes head flits and invalidates the routing tables is set to "on." This informs the Up*/Down* routing table block (Fig. 5-(a)) to discard the information currently held in it. The input buffers and injection ports are also stopped from forwarding/injecting packets into the network. During this recovering state and the initial DRF flag reception at each node in the network, the Up*/Down* logic block is utilized by the root node and the subsequent nodes to mark their output and input ports as either "up" or "down" according to the route reconfiguration rules detailed in Section II-D. The flag forwarding logic and output port status signals (Fig. 5-(c)) co-operate to determine when and what kind of flag (DRF or AF) needs to be forwarded to each direction according to (1) the Up*/Down* logic values and marking scheme (refer to Section II-D), and (2) link statuses (refer to Section II-B).

The four input 1-bit flag wire signals (see Fig. 5-(c)) each direct the Up*/Down* marking in their respective cardinal direction (N, S, E, or W). The output port status identifies the

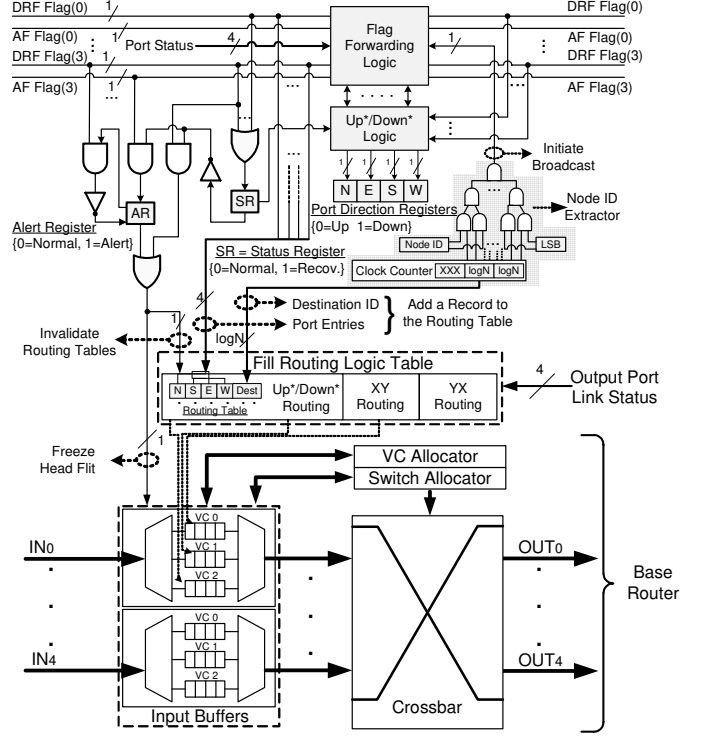


Fig. 4. Schematic of an input-buffered wormhole flow-control router architecture with virtual channels incorporating Hermes components.

health state of each output port; in case the port is non-healthy, i.e., faulty, then the AF flag is forwarded to the adjoining node, otherwise the DRF flag is forwarded (see Section II-D). The DRF flags are received by the routing table filling logic (Fig. 5-(b)), and along with the extraction of the broadcasting node's ID and the direction of the input port(s) from which the DRF flag(s) was received, the corresponding entry in the routing table is updated using one-hot encoding to designate the cardinal direction. The table consists of N 4-bit entries. An entry is recorded once per route reconfiguration process and may only be re-recorded when a later faulty link is detected in the NoC which initiates a fresh route re-discovery process.

B. Node ID Extractor

The Node ID Extractor, depicted in Fig. 4, comprises the hardware which identifies the currently broadcasting node during a route reconfiguration process. It uses a set of $2\log_2(N)$ bits, where N is the number of nodes in the NoC, with its $\log_2(N)$ first LSBs being used to sync to the current $\log_2(N)$ lower bits of the global clock so as to designate the broadcasting cycle of each node, while the $\log_2(N)$ next higher bits are used to identify the flag-broadcasting node (see Section II-D). As a demonstrating example, Fig. 5-(d) presents such hardware (see Section II-C), assuming a four-node 2×2 mesh network. The first two ($\log_2(N = 4) = 2$) Least Significant Bits (LSBs) indicate the broadcasting cycle number, and the next 2 bits indicate which node is broadcasting during the current topology-scanning flag transmission window. For each individual node the node ID is unique (Fig. 5-(d)); hence, when the cycle number equals to the hard-coded node ID, then that node is allowed to broadcast, i.e., nodes 0 and 1 each broadcast when $bit\{3,2\} = \{0,0\}$ and $bit\{3,2\} = \{0,1\}$, respectively, and so on. This process continues until all nodes

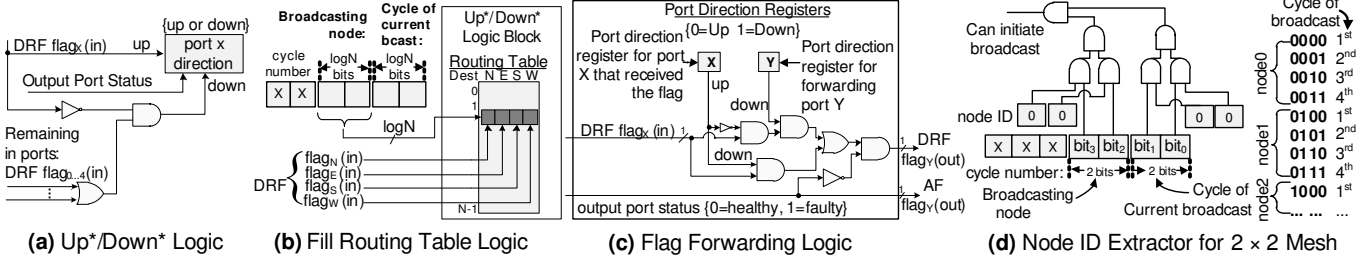


Fig. 5. Schematics of all Hermes's router logic blocks.

finally broadcast their flags during a route reconfiguration process which lasts for N^2 cycles at max (see Section II-B).

IV. EXPERIMENTAL SETUP AND RESULTS

To evaluate Hermes's performance we implemented a detailed cycle-accurate simulator that supports 2D meshes with four-stage pipelined routers (see Section 4), each with 1 to 3 VCs per input port each consisting of 5-flit buffers. Our framework utilizes (a) synthetic Uniform Random (UR) traffic where all nodes have an equal probability of sending/receiving a packet per unit time, (b) Transpose (TR) traffic where packet source and destination coordinates matrix-alternate, an adversarial NoC-stressing form of traffic, and (c) real application workloads. The latter traffic traces are gathered from multi-threaded application execution in a full-system simulation environment, specifically from the Netrace benchmark suite [19], with their packets maintaining dependencies among them, tracked by our simulator for accuracy and fidelity. Synthetic traces, with six-flit 128-bit packets, are run for a million clock cycles, while in Netrace applications results were gathered within a 150-million cycle "region of interest." All experiments were run using an 8×8 2D mesh NoC topology.

Next, two distinct faulty link spatial topology-placing scenarios were utilized in tandem with said traffic patterns: (a) fully random, where all link faults are purely randomly distributed in the NoC's topology, and (b) Hotspot (HS), where half of the faulty links are randomly placed within a 4×4 2D sub-mesh area centrally positioned within the 8×8 2D mesh topology, covering 25% of the NoC's space; the rest of the interconnect faults are randomly mapped onto the remaining network links outside this "hotspot" area. Hence, the hotspot area exhibits a $4 \times$ faulty links density vs. the peripheral NoC area encompassing the rest of the 48 routers, purposely stressing Hermes's robustness capability in detrimental conditions.

Under both faulty link distributions, full topology connectivity was maintained. For fairness, 50 experiments were repeated for each simulation point, to even-out the idiosyncrasy of each individual spatial fault placement, with results averaged. As stated in Section I-A, gate-level faults that render portions of a router as non-functional excite relevant link-level faults. A range of network faulty link counts was considered, up to a severe $> 12\%$ faulty NoC links; though such scenario is extreme, failure probabilities have only been *predicted* for some circuit primitives in future aggressive CMOS technology nodes [33], hence the only scope here is to stress-test Hermes. We compare Hermes against Ariadne [1] and uDIREC [22] which also utilize Up*/Down* routing in NoCs, with both shown to outperform advanced FT schemes such as ImmuneNet [27] and

Vicis [15]. We note that Ariadne's syntectic traffic pattern results reported in the original paper [1] may differ slightly from our results (see Section IV-A) due to idiosyncrasies inherent in link fault placements and traffic patterns.

A. Results With Random Faulty Link Placement

Fig. 6 shows latency-throughput results under UR traffic, using 1 to 3 VCs per port for all considered routing schemes. Under all faulty link density scenarios, all Hermes variants outperform all 3 Ariadne variants (i.e., 1-3 VCs per port) due to the fact that Ariadne's heavy victimization of healthy bidirectional links in enforcing Up*/Down* routing rules in pursue of deadlock-freedom compromises NoC performance.

For up to 5.36% faulty links in the topology all Hermes variants with 2 VCs per port outperform uDIREC with 3 VCs per port. This shows that *VC classification* in terms of a routing path's state, i.e., whether it contains healthy links only (i.e., Hermes uses either XY or O1TURN) or faulty links as well (i.e., Hermes uses Up*/Down* only), is *superior when compared to the arbitrary use of unclassified VCs by a single routing scheme* (i.e., the exclusive use of Up*/Down* by either Ariadne or uDIREC) irrespective whether in-transit messages traverse healthy paths or bypass faulty paths. Under 10.27% or 12.05% faulty links, H-XY with 2 VCs performs equally to uDIREC using 3 VCs. Evidently, under UR traffic, the performance of all six Hermes variants degrades gracefully in terms of the achieved saturation throughput with increasing faulty links count. Further, with just one faulty link present in the entire topology, its negative performance impact under Hermes is constrained, as opposed to the cases of using Ariadne or uDIREC where the attained saturation throughput is reduced dramatically. Indicatively, under 5.36% faulty links H-XY and H-uXY, with each utilizing 2 VCs per port, outperform Ariadne and uDIREC, again with each utilizing 2 VCs per port, by 39.6% and 12.8%, and by 56.4% and 26.4%, respectively. Under the same faulty links setup, H-XY and H-uXY with each utilizing 3 VCs per port, exceed Ariadne and uDIREC, again with each utilizing 3 VCs per port, by 28.7% and 7.2%, and by 49.6% and 24.6%, respectively, while H-O1TURN outperforms Ariadne with 3 VCs by 35.7% and H-uO1TURN tops uDIREC with 3 VCs by 31.2%.

Fig. 7 shows latency-throughput results under TR traffic, using 1 to 3 VCs per port for all examined routing schemes. Again, the performance of all six Hermes variants degrades gracefully in terms of the achievable saturation throughput with increasing faulty links count, and they outperform Ariadne and uDIREC under all equivalent faulty link count scenarios and per-port VC counts. It is also interesting to

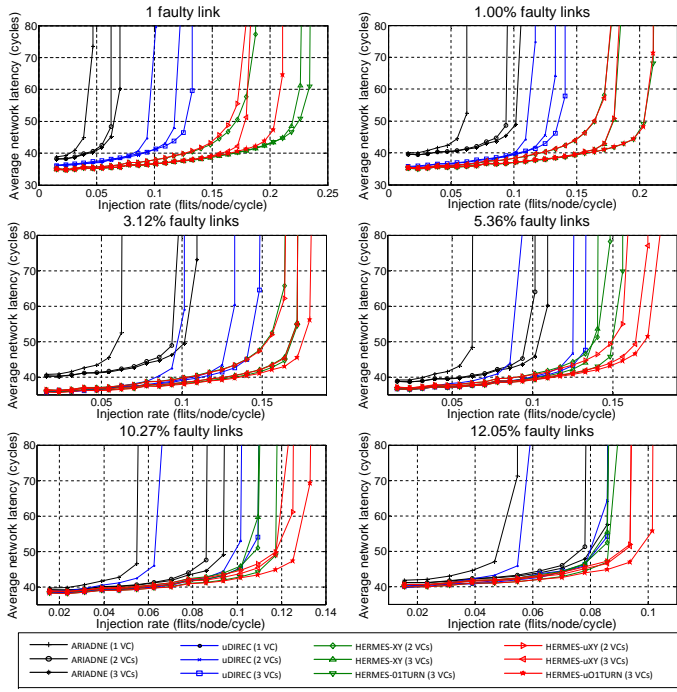


Fig. 6. Latency-throughput curves under a fully random faulty link placement scenario with synthetic uniform random traffic.

see that the non-uDIREC Hermes variants (e.g., H-XY with 3 VCs) actually perform better than the Hermes uDIREC variant counterparts (e.g., H-uXY with 3 VCs); this is due to the fact that the pre-determined routes under uDIREC do not suit non-uniform spatially unbalanced forms of traffic, which overload the network’s virtual diagonals, such as transpose traffic which is utilized here. Indicatively, under 5.36% faulty links, H-uXY (2 VCs) and H-uO1TURN (3 VCs per port) exceed Ariadne and uDIREC, both with 3 VCs, by 41.4% and 57.7%, and 58.6% and 76.9%, respectively. Next, under 10.27% faulty links, H-uXY (2 VCs per port) and H-uO1TURN (3 VCs per port) top Ariadne and uDIREC, with each utilizing 3 VCs per port, by 5.9% and 16.1%, and 39.2% and 52.7%, respectively.

B. Results with Hotspot Faulty Link Placement

The hotspot spatially-distributed faulty link scenario crowds unhealthy links in the topology center to purposely stress Hermes’s robustness capability, as the vertical and horizontal network bisections, which convey most of the mesh’s traffic, overlap perpendicularly in the topology middle. This is even more critical in the case of TR traffic in which all messages traverse the two virtual network diagonals which overlap at the very center of the topology, penetrating the hotspot area.

Fig. 8 and Fig. 9 show latency-throughput results under UR traffic and TR traffic respectively, using 1 to 3 VCs per port for all considered routing schemes. The saturation throughput of all tested routing algorithms, under each respective faulty link density scenario, is higher in the case of UR traffic compared to TR traffic due to said adversarial nature of TR traffic. All uDIREC and Ariadne variants perform worse here (see Fig. 8) as compared to their counterparts under the random faulty links placement using UR traffic in Section IV-A and Fig. 6, as the concentrated faulty links in the topology middle cause excessive re-routing equating to greater hop distances

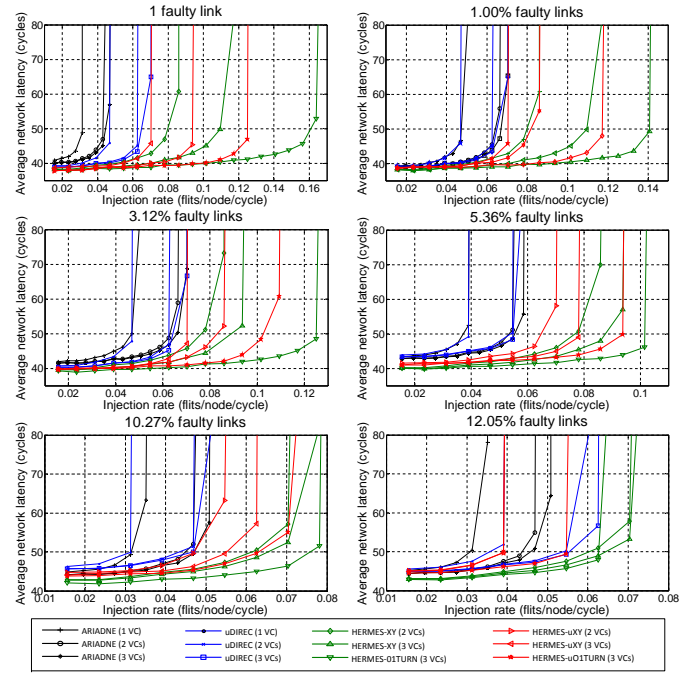


Fig. 7. Latency-throughput curves under a fully random faulty link placement scenario with synthetic transpose traffic.

traversed by messages. Interestingly though, in the case of up to 5.36% faulty links all six Hermes variants perform better than the equivalent experiments carried out in Section IV-A with results shown in Fig. 6. This is because the higher concentration of faulty links in the topology middle leaves fewer faulty links in the periphery of the hotspot area, which captures 75% of the topology, in which either XY or O1TURN routing route efficiently vs. Up*/Down* routing, often utilized in the topology center, which exhibits reduced path diversity. As such, a higher chance in using either XY or O1TURN routing arises, reducing the mean hop distance, hence helping sustain higher network throughput levels.

Such an advantage is diminished at higher faulty link counts, and in all experimental setups where TR traffic is used, i.e., when comparing the results of Fig. 9 to those of Fig. 7, as the combination of unevenly distributed traffic with the nonuniform concentration of faulty links creates highly detrimental to performance conditions. Fig. 9 shows that all Ariadne and H-XY variants perform worse for up to 5.36% faulty links versus the corresponding results of Section IV-A and Fig. 7 where faults are placed randomly. Also, the performance gap between all the Ariadne and uDIREC variants with those of all six Hermes variants is quite large, as shown in Fig. 9. H-O1TURN and H-uO1TURN consistently exhibit the best performance under TR traffic (also for UR traffic) due to the load-balancing nature of O1TURN routing, which proves handy in cases where faults are highly concentrated. Still under TR traffic, at 10.27% and 12.05% faulty link counts the results are slightly smaller, but not too dissimilar, to those of Fig. 7, which shows UR traffic results, for all routing schemes, as due to high fault numbers all algorithms begin to utilize Up*/Down* routing heavily (reduced path diversity). With all schemes utilizing 3 VCs per port and under a single faulty link, H-O1TURN and H-uO1TURN outperform H-XY and Ariadne by 90.9%

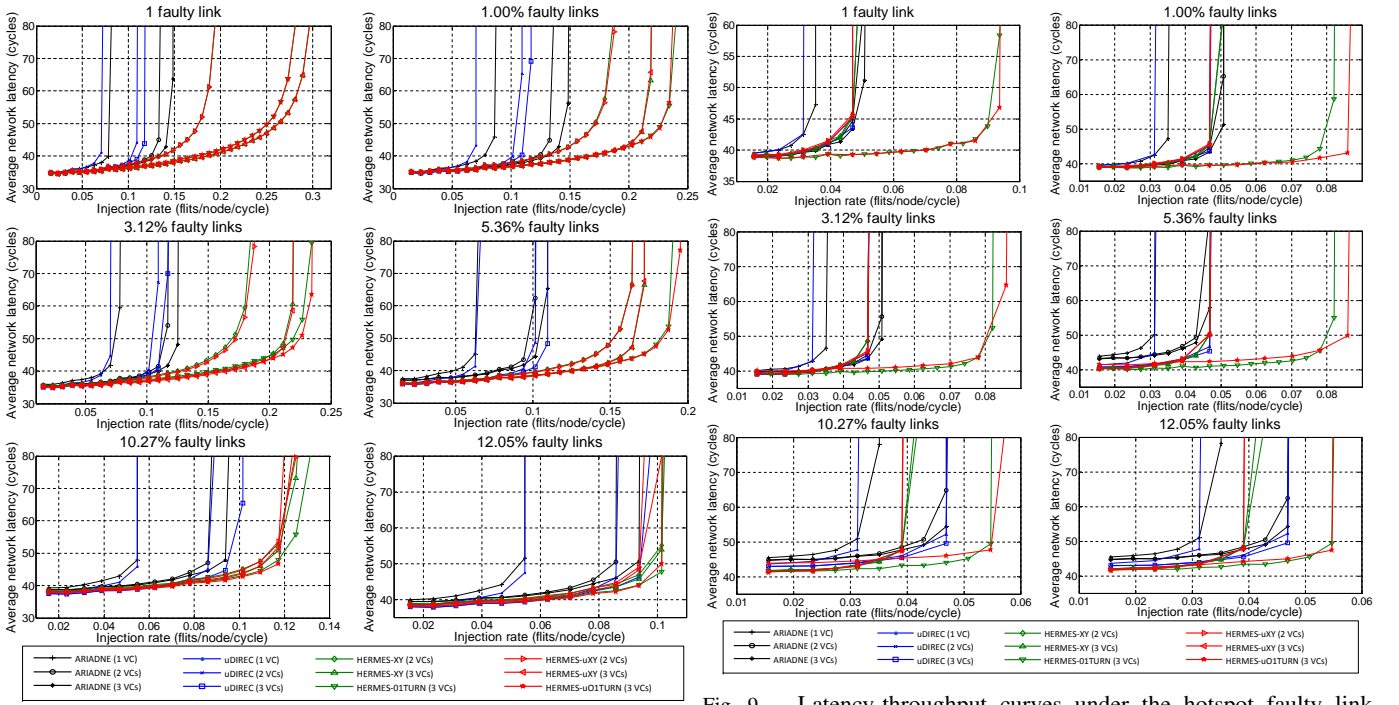


Fig. 8. Latency-throughput curves under the hotspot faulty link placement scenario with synthetic uniform random traffic.

and 133.3%, and 92.4% and 136.8%, respectively, in terms of sustainable throughput, while H-XY outperforms Ariadne by a “mere” 22.2% since H-XY offers no load-balancing. With a greater number of faults present in the topology, the performance of H-XY, H-O1TURN, and H-uO1TURN degrades gracefully. Under the worst-case scenario of 12.05% faulty links, H-O1TURN’s and H-uO1TURN’s throughput are 25.0% and 42.9%, and 26.2% and 44.1% higher than those of H-XY and Ariadne (all with 3 VCs per port), respectively.

C. Realistic Full-System Workload Results

Realistic workload traces were captured from an 8×8 mesh-interconnected CMP running all the multithreaded PARSEC v2.1 suite benchmarks [3] executed onto the M5 simulator [2]. The Netrace infrastructure [19] was used to track dependencies among packetized messages. Each of the 64 tiles contains an in-order Alpha core clocked at 2 GHz, each containing separate 32 KB 4-way set associative L1 I&D caches with 3-cycle access latency with coherency maintained via a MESI protocol, and a 16 MB L2 shared 8-way set associative 64-bank fully-shared S-NUCA with 64 B lines with an 8-cycle access time. Packets consist of 64 bits and 576 bits for miss request/coherence traffic and cache line transfers, respectively. All FT mechanisms use 3 VCs per input port, run using three random faulty link NoC topology placement scenarios: one faulty link, 5.0% and 10.0% NoC faulty links.

Fig. 10 depicts average routing latency results for all Netrace benchmarks. Ariadne and uDIREC are increasingly being outperformed by Hermes’s four variants with growing faulty link counts, showcasing Hermes’s superior performance and robustness attainments. The infusion of the uDIREC scheme in hybrid H-uXY and H-uO1TURN achieves performance gains against H-XY and H-O1TURN respectively, due to the enhanced utilization of unidirectional links and reduced

Fig. 9. Latency-throughput curves under the hotspot faulty link placement scenario with synthetic transpose traffic.

healthy link victimization, with this gap widening under the severe case of 10% faulty links. Indicatively, under 5% faulty links, on average H-XY tops Ariadne and uDIREC by 9.60% and 4.71%, H-O1TURN surpasses Ariadne and uDIREC by 10.66% and 5.83%, H-uXY outperforms H-XY by 3.69% and H-O1TURN by 2.55%, while H-uO1TURN exceeds H-XY and H-O1TURN by 5.12% and 3.99%, all respectively.

D. Zero-Load Latency and Saturation Throughput

An ultra-low injection rate of 0.01 flits/node/cycle is used to emulate zero-load, where 3 VCs per port are used in all tests. Fig. 11-(a) shows that under the use of UR traffic, H-uXY and H-uO1TURN perform identically to uDIREC as the opportunities for route optimization with O1TURN routing are non-existent at zero load. All these three schemes, however, outperform Ariadne, H-XY, and H-O1TURN which victimize a greater number of healthy links due to their bidirectional use of links vs. unidirectional under uDIREC; nevertheless, all routing algorithms, except for Ariadne, perform almost identically for up to ~ 20 faulty links where a relatively limited number of faulty links is encountered across an average path traversed. With one faulty link Ariadne is outperformed by 9.0% by all the other protocols. Under TR traffic, in Fig. 11-(b), interestingly at mid to high fault counts, uDIREC outperforms the remaining schemes due to lesser switching among VCs being carried out when encountering faults, versus all Hermes variants. With 43 faulty links the performance of all algorithms begins to improve due to a more optimal selection of shortest paths picked by the employed Up*/Down* scheme, despite having fewer healthy links available in the topology.

Saturation throughput, here, is considered to be the point where the average NoC latency is $3 \times$ its zero-load latency. All tests carried out utilize 3 VCs per port, with results shown in Fig. 11-(c) and Fig. 11-(d) for respective UR and TR traffic patterns. Under both patterns, Ariadne sustains an

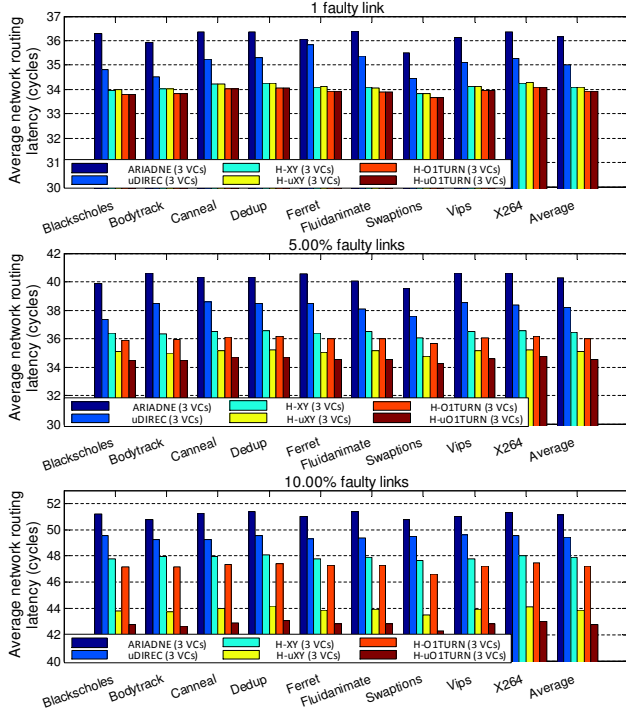


Fig. 10. Network routing latency using the Netrace benchmarks.

almost steady throughput, exhibiting a small degradation at the highest faulty links count end, albeit being at the lowest level vs. all other schemes. This is due to the complete dominance of Up*/Down* routing which victimizes some links as being bidirectionally faulty, severely degrading its performance. uDIREC is the second worst-performing scheme across both UR and TR traffic patterns; it performs slightly better than Ariadne due to its milder link victimization under unidirectional Up*/Down* routing. Interestingly, and consistently, under TR traffic, H-XY outperforms H-uXY, while H-O1TURN outperforms H-uO1TURN, as under uDIREC, the relatively heavier reliance on Up*/Down* routing with fewer links being victimized as faulty, creates elevated congestion vs. alternatively using XY or O1TURN routing. Overall, under both UR and TR, the four Hermes variant schemes are performance-superior to Ariadne and uDIREC. As stated in Section I-A the almost linearly-degrading throughput with an increasing fault links number (an unavoidable phenomenon) sustained by all Hermes variants is an indicator of its near-ideal fault-tolerant routing algorithm nature.

E. Network Response to Dynamically-Occurring Link Faults

We next evaluate Hermes's dynamic behavior in response to real-time fault occurrences in NoC links. As such, we set up a scenario where after an initial stable period of 20,000 cycles, 25 link faults, randomly distributed in the topology, happen concurrently. At that point the entire network's packet flow is frozen and no new packets are network-injected, with flits remaining housed in router injection buffers. The routing tables are invalidated, and the reconfiguration process described in Chapter II is then executed. The network resumes operation after 64^2 (N^2 routers \times N^2 cycles/router; $N = 8$) = 4,096 cycles (at cycle 24,096 in Fig. 11-(e,f)), for the assumed 8-ary 2D mesh NoC, according to timing and syncing requirements of Hermes's reconfiguration algorithm (refer to Section II-C).

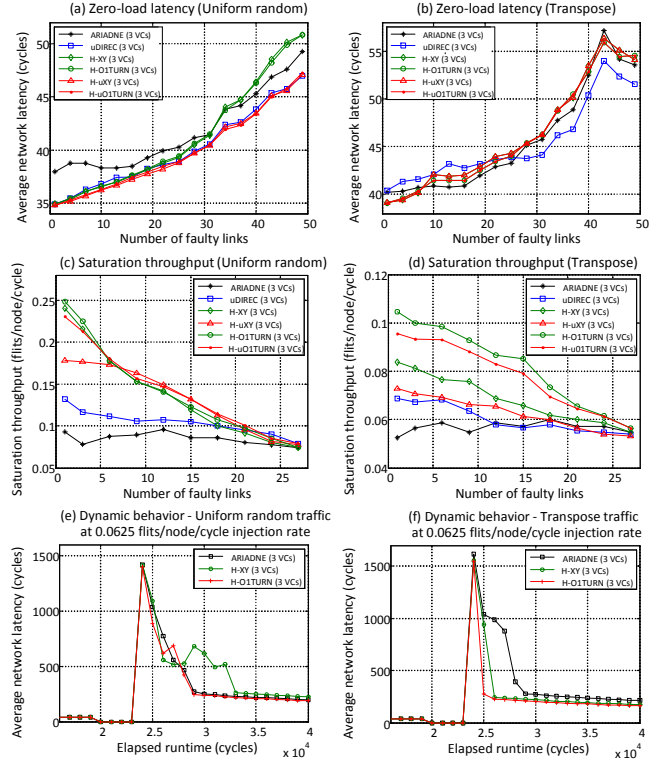


Fig. 11. Zero-Load latency under (a) Uniform Random (UR) and (b) Transpose (TR) traffic patterns, saturation throughput with (c) UR and (d) TR traffic, and network response to dynamic faults: average NoC latency versus time under (e) UR traffic and (f) TR traffic patterns.

Fig. 11-(e) and Fig. 11-(f) show the network reacting to the aforementioned dynamic link faults occurrences scenario under respective UR and TR traffic patterns. Each tested routing algorithm utilizes 3 VCs at each input port, while network latency is measured at 1,000-cycle intervals. A large spike in network latency starts at cycle 20,000, due to the network being frozen awaiting for routing table reconfiguration to complete; this spike is taller under the highly-uneven TR traffic versus UR traffic. As Fig. 11-(e,f), shows, under both said traffic patterns, H-O1TURN takes fewer cycles to stabilize and return to normal NoC latency levels due to its inherent load-balancing routing nature and lower mis-routing rate. Under UR traffic, H-XY spends the longest time to stabilize, due to: (1) the absence of load-balancing, and (2), 180-degree turning when switching from XY to Up*/Down* routing which increases packet hop count. Ariadne, on the other hand, exhibits a more stable behavior since packets follow pre-determined paths. Under TR traffic, Ariadne consumes the most cycles to stabilize its behavior, since it does not feature load-balancing capability, with only one unique path provided between each source-destination router pair, as defined by Up*/Down* routing. As such, these result to higher contention and consequent routing delays across available routing paths.

F. Hardware Synthesis Results

We implemented and synthesized *all the Hermes hardware blocks* illustrated in Fig. 4 and described in Section III using the Synopsys Design Compiler, targeting a commercial 45 nm CMOS technology library at 1 V. We consider three-stage speculative pipelined virtual-channel routers [23] with credit-based wormhole flow-control with a 64-entry SRAM-based

routing table, 128-bit links, 6-flit buffers, 2 GHz clock rate, at 50% switching activity, all for an 8×8 mesh topology. The 2-bit overlay network described in Section II and Section III possesses Triple Modular Redundancy (TMR). Ariadne [1] was also implemented, however the uDIREC reconfiguration scheme [22] is not compared against Hermes as it is heavily dependent on software strategies to form routing paths; in addition, the authors do not specify the implementation of the required end-to-end ECC blocks, and only report area overheads. It is, however expected, that once the reconfiguration hardware, the routing tables and ECC blocks are taken into account, that uDIREC will surpass Hermes's overheads.

Table I briefs power-area overheads for the base speculative NoC router, as well as Ariadne, H-XY and H-O1TURN with 1 up to 3 VCs per input port. H-XY (2 VCs/port) presents 5.31% area and 9.81% power overheads respectively as compared to the base 2 VC per-port NoC router, while the corresponding comparisons against Ariadne with 2 VCs are 0.94% and 4.95%. H-O1TURN (3 VCs/port) presents 4.47% area and 5.91% power overheads respectively as compared to the base 3 VC per-port NoC router, while the analogous comparisons against Ariadne with 3 VCs are 1.51% and 0.47%.

V. BACKGROUND AND RELATED WORK

Fault-Tolerant (FT) approaches applicable to NoCs have been inspired from macro-level Interconnection Networks (INs), where Radetzki's survey [28], and Dally's and Duato's textbooks [7], [12], provide a broad coverage for each respective domain. The scope of any FT approach is universal: to sustain seamless communication among all interconnected entities in the presence of *faulty links*, *faulty nodes*, or *faulty regions*. Duato's landmark work [10] is conducive in developing a theory for FT routing in INs, and consequently NoCs. Essentially, as long as FT routing provides full connectivity devoid of cyclic channel dependencies in a sub-connected (i.e., faulty) topology, then the FT function crucially guarantees deadlock- and livelock-freedom during packet delivery.

Most FT approaches are categorized as: (1) FT routing algorithms (FTRAs) that bypass link/router failures, (2) logic/architectural redundancy within routers to improve their resilience, and, (3) hybrid approaches that combine (1) and (2). Category (1) is further sub-classified as: (a) FTRAs with bounded FT support, (b) FTRAs that sustain unbounded faulty link counts but with spatial pattern limitations, and, (c) FTRAs that bolster unbounded faulty link counts and no spatial placement restrictions. FT schemes in the latter category, e.g., Hermes, are the most flexible, albeit challenging to devise.

The restrictive FT approaches outlined in categories (1-a) and (1-b) above dominated the initial research attempts in INs. Under (1-a), Dally's early reliable router is a 1-FT architecture [8], while the interested reader is urged to refer to related early works found in [7], [12] for holistic coverage. Under category (1-b), in an effort to define permissible spatial fault patterns to avoid deadlocks and simplify FT routing, researchers utilized block-structured shapes, such as convex and/or concave regions of faults, at the expense of victimizing healthy links and routers [38]. Under category (1-c), [16] proposes distributed routing algorithms that re-configure a NoC to

TABLE I
OVERHEADS OF VARIOUS SYNTHESIZED NOC ROUTERS.

Router Virtual Channel Per-Port Count	Router Architecture (128bits)	Area (gates, 1000s)	Power (mW)
1 VC	Base Router	41,98	21,79
	Ariadne	44,64	23,54
2 VCs	Base Router	83,44	33,24
	Ariadne	87,05	34,78
	Hermes-XY	87,87	36,50
3 VCs	Base Router	135,44	56,95
	Ariadne	139,39	60,05
	Hermes-O1TURN	141,50	60,33

avoid faulty components. Next, the Vicis router [15] employs special BIST testers to detect faults, and then leverages extensive re-configurability and an appropriately-designed FTRA to perform port-swapping and crossbar bypassing.

As Hermes reconfigures a faulty topology using Up*/Down* (UD) rules, we next outline the historical timeline of UD routing so as to delineate its evolution. The fundamental work by Perlman [25] presented a self-configuring algorithm that maintains an acyclic spanning subset of a general mesh topology that converges in time proportional to the diameter of its extended LAN. Next, Autonet [32], which comprises a self-configuring LAN, utilizes a distributed algorithm running on switch processors to compute new routes when extra links are incorporated or when existing links fail. Deadlock-free routing and the flooding pattern for broadcast packets in Autonet are both based on computing a spanning tree of operational links inspired from principles outlined in Perlman's algorithm, and extended with the use of the then proposed UD routing which performs BFS from a root node that establishes deadlock freedom and full network connectivity. Next, work by Sancho *et al.* [29], [31] proposed the use of UD routing in NoWs with irregular topologies where deadlock-free routing tables are computed based on Depth-First Search (DFS; instead of BFS) spanning tree generation to eliminate cyclic dependencies where throughput is improved with the use of minimal routes and traffic balancing, albeit with no support for fault tolerance. The same authors also proposed the use of a Flexible Routing scheme [30] applicable to regular networks, i.e., meshes. Following, Silla *et al.* [35] extend the original UD topology-agnostic routing in irregular NoWs and proposed two general methodologies toward the design of high-performance adaptive routing algorithms, albeit with no fault tolerance support.

Topology-agnostic algorithms that discover deadlock-free routes via reconfiguration have also become handy for faulty NoCs. Ariadne's reconfiguration algorithm [1] which uses UD routing to compute routes when faults in links occur was first devised. Next, uDIREC [22] reconfigures routing paths in a faulty NoC by also using UD routing, where an iterative software-based spanning tree kernel utilizes NoC path diversity to optimize routes with restricted unidirectional link victimization vs. Ariadne. Last, Fault- and Application-aware Turn model Extension (FATE) routing [20] also utilizes a topology-agnostic iterative-based software approach to generate a deadlock-free application-aware routing function.

Under category (2), prominently, Bulletproof [6] analyzes the reliability vs. area tradeoffs of various NoC router designs and proposes run-time repair and recovery methodologies at the system-level. Next, [37] makes use of partially faulty links, while [14] converts a uni-directional link to work in a full-

duplex mode in case the node-pairing link fails. Last, under category (3), stochastic communication techniques [13] use probabilistic packet broadcasting schemes to handle faults.

VI. CONCLUSIONS

This paper presented Hermes, a near-ideal, high-throughput, distributed, and deadlock-free FT routing algorithm with high robustness and graceful performance degradation with increasing faulty link counts. Hermes is a hybrid routing scheme: it balances traffic to sustain high performance onto fault-free paths, while it provides pre-configured escape path selection in the vicinity of faults. Hermes improves throughput by up to $3\times$, and is able to identify network segmentations.

REFERENCES

- [1] K. Aisopos *et al.* *ARIADNE: Agnostic Reconfiguration in a Disconnected Network Environment*. Proc. ACM PACT, pp. 298-309, Oct. 2011.
- [2] N.L. Binkert *et al.* *The M5 Simulator: Modeling Networked Systems*. IEEE Micro Magazine, Vol. 26, No. 4, pp. 52-60, July/Aug. 2006.
- [3] C. Bienia *et al.* *The PARSEC Benchmark Suite: Characterization and Architectural Implications*. Proc. ACM PACT, pp. 72-81, Oct. 2008.
- [4] J. R. Black. *Electromigration Failure Modes in Aluminum Metallization for Semiconductor Devices*. Proc. of the IEEE, Vol. 57, No. 8, pp. 1587-1594, Sept. 1969.
- [5] C. Constantinescu. *Trends and Challenges in VLSI Circuit Reliability*. IEEE Micro Magazine, Vol. 23, No. 4, pp. 14-19, July-Aug. 2003.
- [6] K. Constantinides *et al.* *BulletProof: A Defect-Tolerant CMP Switch Architecture*. Proc. IEEE HPCA, pp. 5-16, Feb. 2006.
- [7] W.J. Dally and B. Towles. *Principles and Practices of Interconnection Networks*. Morgan Kaufmann Publishers Inc. ISBN: 9780122007514, 2004.
- [8] W.J. Dally *et al.* *The Reliable Router: A Reliable and High-Performance Communication Substrate for Parallel Computers*. Proc. Int'l Parallel Computer Routing and Commun. Workshop, pp. 241-255, May 1994.
- [9] A. DeOrio *et al.* *DRAIN: Distributed Recovery Architecture for Inaccessible Nodes in Multi-Core Chips*. Proc. DAC, pp. 912-917, June 2011.
- [10] J. Duato. *A Theory of Fault-Tolerant Routing in Wormhole Networks*. IEEE TPDS, Vol. 8, No. 8, pp. 790-802, Aug. 1997.
- [11] J. Duato. *A Necessary and Sufficient Condition for Deadlock-Free Adaptive Routing in Wormhole Networks*. IEEE TPDS, Vol. 6, No. 10, pp.1055-1067, Oct. 1995.
- [12] J. Duato *et al.* *Interconnection Networks: An Engineering Approach*. Morgan Kaufmann. ISBN: 1558608524, 2002.
- [13] T. Dumitras and R. Marculescu. *On-Chip Stochastic Communication*. Proc. DATE, pp. 790-795, Mar. 2003.
- [14] M. A. Al Faruque *et al.* *Configurable Links for Runtime Adaptive On-Chip Communication*. Proc. DATE, pp. 256-261, April 2009.
- [15] D. Fick *et al.* *Vicis: A Reliable Network for Unreliable Silicon*. Proc. DAC, pp. 812-817, July 2009.
- [16] D. Fick *et al.* *A Highly Resilient Routing Algorithm for Fault-Tolerant NoCs*. Proc. DATE, pp. 21-26, April 2009.
- [17] A. Furber. *Living With Failures: Lessons from Nature?* Proc. IEEE ETS, pp. 4-8, May 2006.
- [18] D. Gizopoulos *et al.* *Architectures for Online Error Detection and Recovery in Multicore Processors*. Proc. DATE, Embedded Tutorial, pp. 533-538, April 2011.
- [19] J. Hestness *et al.* *Netrace: Dependency-Driven Trace-Based Network-on-Chip Simulation*. Proc. Int'l Workshop on Network on Chip Architectures, pp. 31-36, Dec. 2010.
- [20] D. Lee *et al.* *Highly Fault-tolerant NoC Routing with Application-Aware Congestion Management*. Proc. IEEE/ACM NOCS, Article Np. 10, pp. 1-8, Sept. 2015.
- [21] R. Marculescu *et al.* *Outstanding Research Problems in NoC Design: System, Microarchitecture, and Circuit Perspectives*. IEEE TCAD, Vol. 28, No. 1, pp. 3-21, January 2009.
- [22] R. Parikh and V. Bertacco. *uDIREC: Unified Diagnosis and Reconfiguration for Frugal Bypass of NoC Faults*. Proc. IEEE/ACM Micro, pp. 148-159, Dec. 2013.
- [23] L.-S. Peh and W. J. Dally. *A Delay Model and Speculative Architecture for Pipelined Routers*. Proc. IEEE HPCA, pp. 255-266, Jan. 2001.
- [24] A. Prodromou *et al.* *NoCAAlert: An On-Line and Real-Time Fault Detection Mechanism for Network-on-Chip Architectures*. Proc. IEEE/ACM Micro, pp. 60-71, Dec. 2012.
- [25] R. Perlman. *An Algorithm for Distributed Computation of a Spanning Tree in an Extended LAN*. In ACM SIGCOMM Computer Communication Review, Vol. 15, No. 4, pp. 44-53, Sept. 1985.
- [26] M.D. Powell *et al.* *Architectural Core Salvaging in a Multi-Core Processor for Hard-Error Tolerance*. Proc. IEEE/ACM ISCA, pp. 93-104, June 2009.
- [27] V. Puente *et al.* *Immunet: A Cheap and Robust Fault-Tolerant Packet Routing Mechanism*. ACM SIGArch Computer Architecture News, Vol. 32, No. 2, pp. 198-209, March 2004.
- [28] M. Radetzki *et al.* *Methods for Fault Tolerance in Networks-on-Chip*. In ACM Computing Surveys (CSUR), Vol. 46, No. 1, Article No. 8, Oct. 2013.
- [29] J.C. Sancho *et al.* *A New Methodology to Compute Deadlock-Free Routing Tables for Irregular Networks*. Proc. Workshop Comm., Architecture and Applications for Network-Based Parallel Computing (CANPC), pp. 45-60, Jan. 2000.
- [30] J.C. Sancho *et al.* *A Flexible Routing Scheme for Networks of Workstations*. Proc. 3rd Int'l Symp. High Performance Computing (ISHPC), pp. 260-267, Oct. 2000.
- [31] J.C. Sancho *et al.* *An Effective Methodology to Improve the Performance of the Up*/Down* Routing Algorithm*. IEEE TPDS, Vol. 15, No. 8, pp. 740-754, Aug. 2004.
- [32] M.D. Schroeder *et al.* *Autonet: A High-Speed, Self-Configuring Local Area Network Using Point-to-Point Links*. IEEE J. Selected Areas in Comm., Vol. 9, No. 8, pp. 1318-1335, Oct. 1991.
- [33] Semiconductor Industry Association, 2014. Int'l Technology Roadmap for Semiconductors. Available [online]: <http://www.itrs.net/reports.html>
- [34] D. Seo *et al.* *Near-Optimal Worst-Case Throughput Routing for Two Dimensional Mesh Networks*. Proc. IEEE/ACM ISCA, pp. 432-443, June 2005.
- [35] F. Silla and J. Duato. *High-Performance Routing in Networks of Workstations with Irregular Topology*. IEEE TPDS, Vol. 11, No. 7, pp. 699-719, August 2002.
- [36] S. R. Vangal *et al.* *An 80-Tile Sub-100-W TeraFLOPS Processor in 65-nm CMOS*. IEEE JSSC, Vol. 43, No. 1, pp. 29-41, Jan. 2008.
- [37] A. Vitkovskiy *et al.* *A Dynamically Adjusting Gracefully Degrading Link-Level Fault-Tolerant Mechanism for NoCs*. IEEE TCAD, Vol. 31, No. 8, pp. 1235-1248, Aug. 2012.
- [38] J. Wu. *A Fault-Tolerant and Deadlock-Free Routing Protocol in 2D Meshes Based on Odd-Even Turn Model*. IEEE TOC, Vol. 52, No. 9, pp. 1154-1169 Sept. 2003.



on-chip networks.



View CA as a senior software engineer.

Costas Iordanou received the B.Sc. (2013) and M.Sc. (2014) degrees in Computer Engineering and Informatics from the Cyprus University of Technology. He also holds a M.Sc. degree in Telematic Engineering from Universidad Carlos III de Madrid (2015). Currently he is working on completing his Ph.D. degree (Marie Curie, ITN-METRICS program) at the Universidad Carlos III de Madrid in collaboration with Telefonica I + D. His research interests focus on targeted web advertising, web tracking, online price discrimination, and fault-tolerant

Vassos Soteriou received the B.S. and Ph.D. degrees in electrical engineering from Rice University, Houston, TX, in 2001, and Princeton University, Princeton, NJ, in 2006, respectively. He is currently an Associate Professor at the Department of Electrical Engineering, Computer Engineering and Informatics at the Cyprus University of Technology. He is a recipient of a Best Paper Award at the 2004 IEEE International Conference on Computer Design. His research interests lie in multicore computer architectures, and on-chip networks.

Konstantinos Aisopos received his PhD degree from Princeton University in 2012. His research has been on on-chip networks and reliability. During his Ph.D. studies, he spent three years at MIT, developing a circuit-level accurate fault-modelling tool for on-chip routers. He then spent five years at Microsoft Seattle, working on Cortana and developing an artificially intelligent digital assistant for Windows. During 2017-2019, he co-founded a startup on Machine Learning in Davis, CA. Since 2019 he has been working at Google in Mountain